9-1-2016

A Multi-Wavelength Analysis of Cold Evolving Interstellar Clouds

Mary Spraggs
Western Kentucky University, mary.spraggs727@topper.wku.edu

A MULTI-WAVELENGTH ANALYSIS OF COLD EVOLVING INTERSTELLAR CLOUDS

A Capstone Experience/Thesis Project

Presented in Partial Fulfillment of the Requirements for

the Degree of Bachelors of Science with

Honors College Graduate Distinction at Western Kentucky University

By
Mary Elizabeth Spraggs

*****

Western Kentucky University
2016

CE/T Committee:

Dr. Steven Gibson, Advisor

Dr. Doug Harper

Dr. Elizabeth Gish

Approved by

_____
Advisor
Department of Physics & Astronomy

ABSTRACT

The interstellar medium (ISM) is the dynamic system of gas and dust that fills the space between the stars within galaxies. Due to its integral role in star formation and galactic structure, it is important to understand how the ISM itself evolves over time, including the process of cooling and condensing required to form new stars. This work aims to constrain and better understand the physical properties of the cold ISM with several different types of data, including large surveys of neutral atomic hydrogen (HI) 21cm spectral line emission and absorption, carbon monoxide (CO) 2.6mm line emission, and multi-band infrared dust thermal continuum emission. We are developing an algorithm that identifies areas where the gas may be cooling and forming molecules using HI self-absorption, in which a cold foreground HI cloud absorbs radiation from warmer background HI emission, and analyzes the HI spectral line in parallel with the CO and infrared data. From these inputs, the algorithm can determine the gas temperature, density, molecular abundance, and other properties as functions of position.

Keywords: interstellar medium, astrophysics, galactic evolution, physics

ACKNOWLEDGEMENTS

Generous funding by the Honors College via the Gatton Academy Alumni Grant is greatly appreciated. Other funding sources include the WKU Department of Physics & Astronomy, the Ogden College of Science & Engineering, the NASA Kentucky Space Grant Consortium, and the National Science Foundation.

VITA

1994	Born - Valparaiso, IN
2013	Carol Martin Gatton Academy of Mathematics & Science Bowling Green, KY
2014	Intern at the Massachusetts Institute of Technology's Haystack Observatory
2015	Intern at the National Astronomy and Ionosphere Center (Arecibo Observatory)
2016	University of Wisconsin Madison

FIELDS OF STUDY

Major Field: Physics

Minor Field: Mathematics

TABLE OF CONTENTS

LIST OF FIGURES

CHAPTER 1

INTRODUCTION

Our 13.8 billion year old universe contains an estimated 100 billion galaxies, which are gravitationally bound systems of stars, gas, dust, and dark matter with diverse shapes and structures. The Milky Way Galaxy, our home, is a barred spiral galaxy with several hundred billion stars, with our solar system being roughly 30,000 light years from the center by the best current estimates. Our Galaxy's gas and dust, referred to as the interstellar medium (ISM), is an incredibly complex and dynamic system that plays a direct role in star formation and galactic evolution (Ferriere 2001; Draine 2011). The ISM consists of different types of monatomic and molecular gases and ash-like dust particles distributed within a wide variety of filamentary, sheetlike, and other topological structures whose densities rarely exceed those of the best terrestrial vacuum chambers. Since it is so widespread, the ISM is found in a variety of environments, ranging from relatively cold, dense clumps to hot, tenuous clouds, some of whose properties are listed in Table 1. The densest ISM clouds can serve as stellar nurseries. Ultimately, the ISM is the source of all the Galaxy's stars and the heavier elements they produce via nuclear fusion, without which life-supporting planets like our own would not exist. This thesis examines the properties of cold clouds that may be evolving toward a physical state where stars can form

As shown in Table 2, most interstellar matter (and consequently most stellar material) is hydrogen, a primordial gas produced in the Big Bang. Thus it is useful to consider the content and structure of ISM clouds in terms of hydrogen gas,which has neutral atomic, diatomic molecular (H_2), and ionized forms. Neutral atomic hydrogen (HI) is the most easily observed phase, thanks to its prominent 21 cm emission spectral line. As with other spectral lines, the HI 21 cm line can manifest as either as emission or absorption, with the latter arising when an HI atom "consumes" a photon of the right energy to excite it, with this being more likely for colder HI gas. Absorption requires a bright source of background radiation, usually 21 cm continuum from a distant quasar or supernova remnant. However, 21 cm line emission from a warmer background HI cloud will also suffice, in which case the phenomenon of HI self-absorption (HISA) occurs (Gibson 2010). HISA's need for bright background HI emission at the same Doppler velocity as the foreground absorbing cloud makes it very rare in most parts of the sky but is fairly common near the Galactic plane, where most interstellar matter is found. The requirements for HISA to appear also provide interesting constraints on the physical properties of the absorbing clouds, such as their temperatures and densities, and even their balance of atomic and molecular hydrogen.

Molecular hydrogen, as another major form of hydrogen in the Galaxy, is important in its own right as the most abundant molecule in space. However, unlike its atomic counterpart, H_2 is very delicate and can be dissociated by UV photons from stars. Usually, it only forms in cold, dense clouds that are shielded by shells of HI and dust. Interstellar dust, which is ubiquitous throughout space, can also enhance the formation of H_2 by providing a surface for hydrogen atoms to attach to electrically, which increases

the chance of collisions significantly compared to free interstellar atoms. However, because H_2 tends to form in cold pockets of clouds where it is shielded, it is difficult to observe directly, as it only emits radiation at higher temperatures. In order to know how much H_2 is present, one must find a tracer: another interstellar molecule whose abundance is assumed to be proportional to that of molecular hydrogen. Carbon monoxide (CO) is most commonly used. Its brightest (J = 1 -> 0) transition emits at a wavelength of 2.6 mm.

CO has its limitations: it requires the presence of H_2 in order to provide a chemical pathway for its formation and to shield it from dissociation by interstellar high-energy photons. Molecular hydrogen does not have corresponding restrictions, so while CO must have H_2 present, some H_2 may very well exist without CO and be undetectable with the CO tracer (Grenier et al. 2005; Douglas & Taylor 2007). To account for this "missing" portion of diffuse H_2 a different approach must be taken, which is a major component of this project. For an explanation of diffuse H_2 and other components of the hydrogen budget, see Table 1.

The reason we must account for this dark H_2 is to learn how much hydrogen is present in all cloud forms. This amount is measured in terms of column density, the number of particles per unit area summed over the distance between the observer and the object; column density and other physical parameters are listed in Table 2. Column density is often easily obtained by simply rescaling the observed brightness values, which is the first step in determining other cloud properties, as will be explained in later sections. My analysis generates a set of different maps showing gas property values at different locations within a HISA cloud. These property maps will allow understanding of how

cloud properties depend on location within the Galaxy as well as the evolution of a particular cloud.

Phase	**Temperature (K)**	**Particle Density (cm^{-3})**	**Sample Tracer**	**Description**
Warm Neutral Medium	~5000	~0.5	HI 21 cm emission line	Almost entirely atomic gas heated by stellar radiation
Cool Neutral Medium	~30-80	~50-100	HI 21 cm emission and absorption	Predominantly HI, in irregularly shaped clouds
Diffuse H_2	~15-50	~60-200	minimal CO; infrared dust	Irregularly shaped clouds, several parsecs in length
Dense H_2	~10-50	$>10^4$	CO and other molecule emission lines	Roughly spherical clouds, much smaller than diffuse clouds

Table 1. Some of the major phases of the ISM. This is not a complete summary, as the ISM can be characterized by a variety of parameters, the transition between phases is not always clear, and because there are other phases (Draine 2011; Ferriere 2001; Carroll & Ostlie 2007).

Material	Particle Abundance	Abundance by Mass
Hydrogen (H_2 + HI + HII)	90.8%	70.4%
Helium (He)	9.10%	28.1%
Heavier Elements	0.12%	1.50%

Table 2. Hydrogen gas makes up the largest portion of the ISM. This hydrogen was formed in the Big Bang along with most of the helium. The amount of hydrogen has decreased slightly due to the formation of stars: nuclear fusion within stellar interiors has lead to the increase in the amount of helium and the formation of heavier elements.
Approximately half of the heavier material is estimated to be in the form of solid dust particles. (Ferriere 2001)

Property	**Symbol**	**Range**	**Units**	**Description**
Fractional Abundance (HI)	f	0-1	Unitless	Fraction of free particles that are HI
Column Density	N	~10^{19}-10^{22}	cm^{-2}	Integrated number of particles per unit area
Particle Density	n	~1-10^{6}	cm^{-3}	Number of particles per unit volume
Optical Depth	**τ** (Greek tau)	a few	Unitless	Transparency of an object to radiation (0 means transparent, 1 is opaque)
Background Fraction	p	0-1	Unitless	Fraction of total HI emission coming from behind a cloud

Table 3. The values of some of the major parameters of the ISM vary greatly in magnitude, and even though space is better than any vacuum that can be produced on Earth, the number of particles over an integrated distance per area (column density) can be very high due to the distances involved and because colder clouds are more dense.

CHAPTER 2

DATA

2.1 Overview of Data

A major strength of this study is its use of multiple datasets tracing different constituents of the cold neutral ISM to better understand each cloud's evolution and current state. Handling multiple datasets from different surveys is difficult but allows the best available data to be used for each target. To compare one survey to another, the spectral-line data must be integrated over frequency, and all images must be convolved to the same angular resolution and converted to a common set of units measuring the quantity of gas at each position. The processing of the data is the topic of this section, preceded by a description of the original dataset and the facility that performed the original observations.

The HI data comes from the Canadian Galactic Plan Survey (CGPS; Taylor et al. 2003), which was observed with the Dominion Radio Astrophysical Observatory's Synthesis Telescope, an interferometer array of seven radio dishes located in the Canadian province of British Columbia. The CGPS covers a large portion of the Milky Way Galaxy at 1 arc-minute angular resolution with a series of overlapping "spectral-line image cubes" showing HI line emission brightness as a function of Galactic longitude,

latitude, and redial velocity along the line of sight translated from observed frequency by the Doppler shift from the gas motion relative to the observer. While not designed to study HISA specifically, the CGPS has proved useful in identifying smaller features in the HI emission with much more intricate detail than previous surveys (Gibson et al. 2000). The CGPS was completed in multiple phases, with Phase I covering Galactic longitudes between 74.2^{o} and 147.3^{o} and latitudes from -3.6^{o} to +5.6^{o}. Initially, a well known HISA feature at longitude 139^{o} and latitude -1^{o} was studied in detail, but testing how well the algorithm handled a variety of other locations and environments was required. A so called "supermosaic," a large image created from several smaller ones, was created and encompassed longitudes 146^{o} - 136^{o} and latitudes -3^{o} - +5^{o}.

HISA features were detected in the CGPS data with an algorithm that searches for local minima in emission maps with a matching narrow, sharp dip in the spectral line (Gibson et al. 2005a,b). This algorithm cannot locate HISA where it is not detectable: when a cloud has either too low column density or is too diffuse. Despite these limitations, the algorithm still finds many HISA features that can be further studied in this project. As mentioned previously, since HISA is a phenomenon that is seen in cold gas, molecules such as carbon monoxide and molecular hydrogen are likely to form in close proximity where they can be shielded by denser material.

The Outer Galaxy Survey (OGS; Heyer et al. 1998) provides high quality image cubes of CO in a large portion of the CGPS coverage area and is particularly well suited for studying the relationship between molecular and atomic gases found in interstellar clouds. The survey was taken by the now-decommissioned Five College Astronomy Ob-

servatory 14 m telescope near New Salem, Massachusetts and covered Galactic longitudes 102.49^{o} to 141.45^{o} and Galactic latitudes -3.03^{o} to 5.41^{o}. Within this region in the outer Milky Way, a variety of environments and structures are captured, and since the outer region of the Galaxy contains less emission features than the more crowded inner region, the clouds themselves and their properties are more easily defined. The original OGS data contained many gaps near the edge of the survey area and was supplemented with Extended Outer Galaxy Survey (Brunt et al., in prep). Both surveys are very similar, with resolutions of 45 arc-seconds, and were combined with a C program that averages overlapping images to produce a larger one.

The *Planck* satellite provides 2-D maps of infrared thermal dust continuum emission with a resolution of five arc-minutes (Planck Collaboration 2014). This satellite was operated by the European Space Agency between its startup in 2009 until its deactivation in 2013. Originally designed to study the structure and evolution of the universe using the cosmic microwave background radiation, the satellite also measured thermal emission heated by starlight to see the overall distribution of ambient interstellar material. To complete its primary goals, the project collected data for the entire sky, and the sensitivity and frequency range of *Planck* allows it to detect most cold dust emission, which is of great utility for studying the ISM's structure and properties. The particular *Planck* data product used here is a map of total dust emission at each position on the sky, which can be used as a proxy for total gas content if the gas and dust are uniformly mixed.

2.2 Data Preparation

Each data set, the HI from the CGPS, CO from EOGS and OGS, and dust from *Planck*, was different from the others in terms of raw units, quality, and resolution. For any type of comparative analysis to occur, the data had to be put into to a similar form in terms of units and dimensions. This was done with two pre-existing C programs. The first simply summed up the brightness over all velocity channels for each separate position on the sky, thereby converting a 3-D data cube into a 2-D map. This is a necessary step for the three dimensional HI and CO data, since the *Planck* dust maps already show emission for all velocities.

Since both the CGPS and OGS/EOGS surveys have much sharper resolutions than the *Planck* data, they also had to be convolved with a circularly symmetric Gaussian function to "blur" them to the same resolution as the dust data.

The final step was to convert each HI, CO, and dust map into different units of column density (the number of particles per unit area) by using different conversion factors for each ISM constituent. The conversion factor for HI is $1.823*10^{18}$ cm^{-2} (K km/s) (Dickey and Lockman 1990), the CO factor is $1.8*10^{20}$ cm^{-2} (K km/s) (Dame et al. 2001), and the dust conversion is $5.8*10^{21}$ cm^{-2} mag^{-1} (Bohlin 1978). Each conversion factor scales the given data values into the proper value and units for column density. The products of this preparation are shown in Figs. 1, 2, and 3.

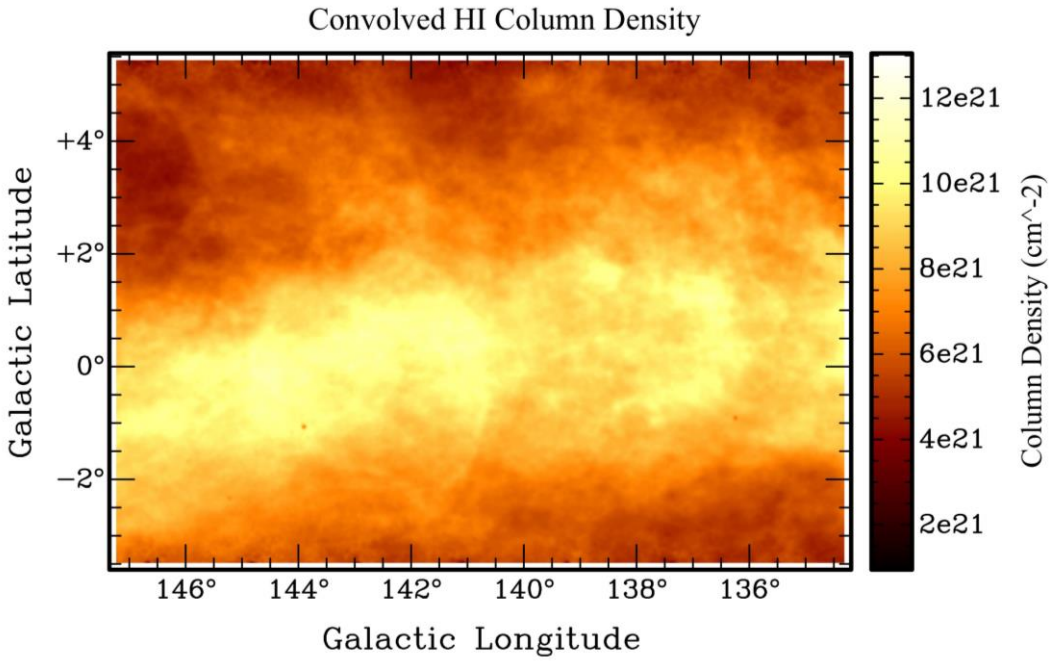

Figure 1. The convolved column density supermosaic of CGPS HI emission that is used by the algorithm. This map was made from six smaller images that were first integrated and then convolved in order to match the resolution of the *Planck* dust data. This region lies in the plane of the Galaxy, about 140° away from the Galactic center direction.

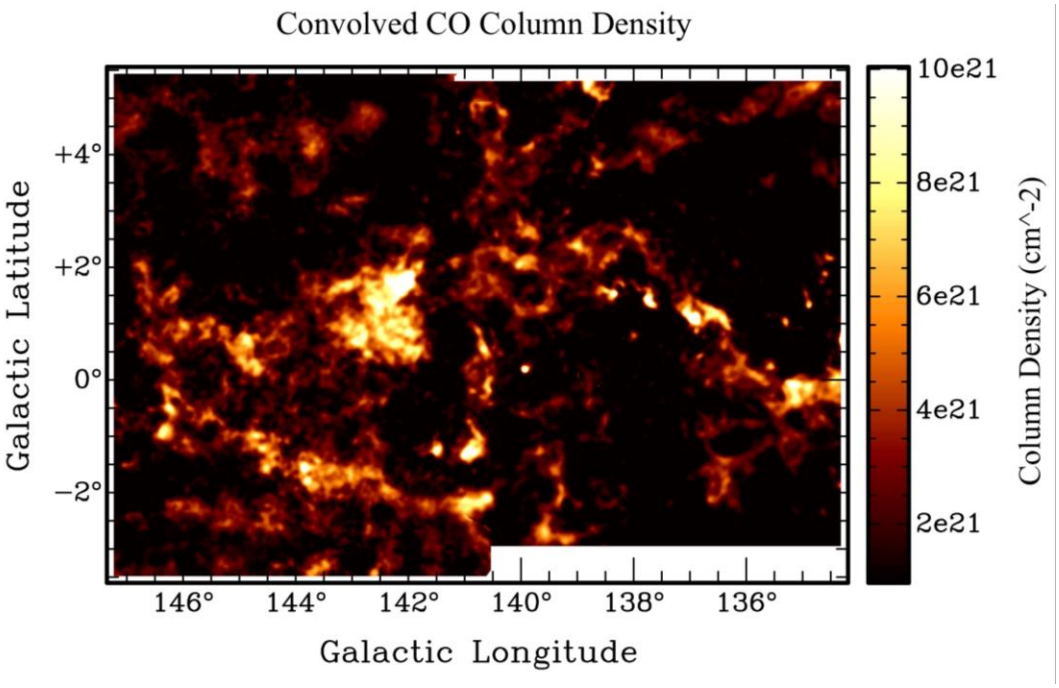

Figure 2. An example of a CO supermosaic for the same region in Fig. 2. The creation of this map involved an extra step, in which the OGS and EOGS images were combined to improve sky coverage.

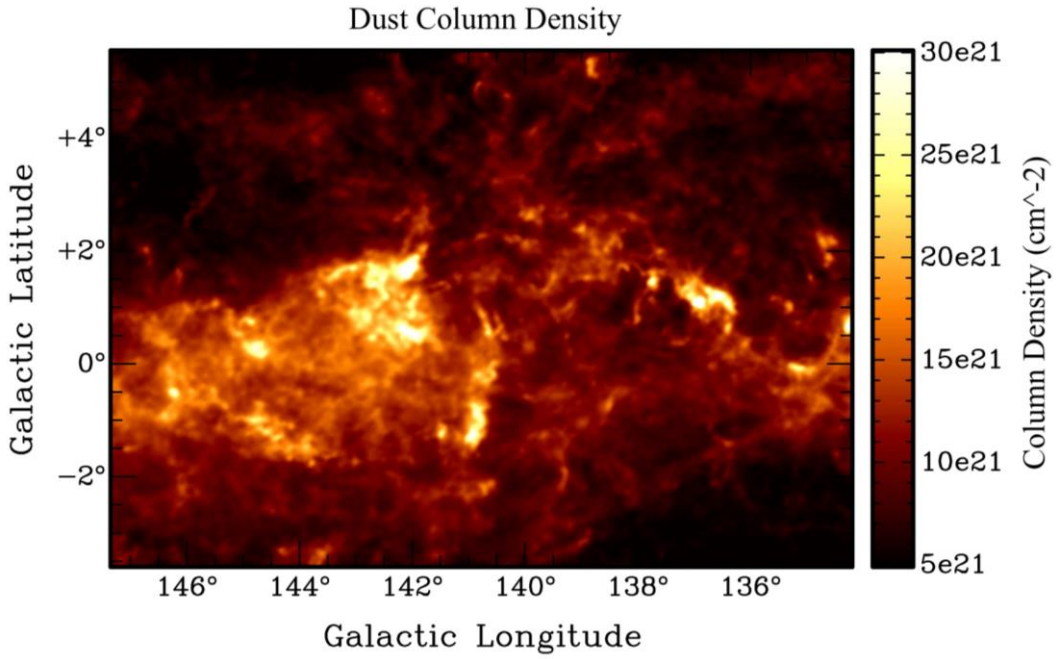

Figure 3. The matching supermosaic of *Planck* infrared dust emission. This dust is used as an ambient tracer for all interstellar matter, including any dark material of the ISM that is not directly observable using normal HI and CO emission.

CHAPTER 3

DATA ANALYSIS

3.1 Dark Molecular Hydrogen

The amount of dark H_2 must first be determined before any significant constraints can be placed on the physical parameters of the HISA clouds. In most other studies focusing on HISA clouds and their properties (Feldt 1993; Kavars et al. 2003), the column density of dark H_2 is generally considered to be insignificant and ignored. This work does not follow that assumption and shows that the column density of dark H_2 is a critical piece of information for acquiring the best possible HISA parameter constraints (Grenier et al. 2005).

The multi-wavelength and multiple data source aspect of this project is a major strength since the column of dark molecular hydrogen (and some HISA) can best be determined indirectly by removing the known amount of material in the hydrogen budget from the total column traced by dust. Since the HI emission shows all of the obvious neural atomic gas and the CO traced the observable molecular material, subtracting those components from the dust yields the dark gas content. Preliminary results suggest that the order of magnitude is around 10^{20} to 10^{21} cm^{-2} , which rivals that of other major ISM

constituents. With knowledge of the column density for both varieties of hydrogen found in the cold phase of the ISM, further properties can be derived.

3.2 Determination of HISA Areas

In addition to the processing of the ISM constituent data, maps of HISA have used that were previously identified by Gibson et al. (2005a,b). The HISA features' brightness temperature maps (Fig. 4) can be used to create zone maps (Fig. 5), which are essential in the proper execution of the algorithm because they mark out HISA regions, a buffer zone, a so-called "NEAR-OFF" region, and OFF HISA areas, and positions where there is no available data.

The zone maps are made in a relatively straightforward way: the brightness temperature map of HISA for a particular region like that shown in Fig. 4 is read into a code that moves through the image pixel by pixel and flags those that contain a data value less than 0 K (the brightness temperature is negative because HISA is absorption). The code then assigns these points, which mark the location of HISA features, an integer value of 1, to indicate that they are ON positions.

Next, a region one CGPS beam width wide, or 1 arc-minute (3.3 pixels), was selected in a similar manner. The pixels in the HISA map that were within the one beam width distance were marked in the blank image with a value of 2 and represent the first of two zones that are extensions of the HISA area. This first one is to make sure that any future selection processes that take data from the images truly select regions that are not HISA clouds. The second extensive region is selected in an identical way but surrounds

the buffer zone and the HISA feature. This region marks the region in the HISA maps that is another beam width further off of the clouds. While this NEAR-OFF region does not contain any HISA, it is still expected to be a part of a larger cold, dense cloud system where dark H_2 molecules may exist.

Any region that is not a HISA feature or contained within two beam widths of the HISA is referred to as being an OFF position; these regions are marked colored white in Fig. 5 and data taken from these regions are compared against data associated with HISA features to determine the portion of the total column density contributed by the HISA cloud rather than unrelated gas in from of or behind the HISA cloud.

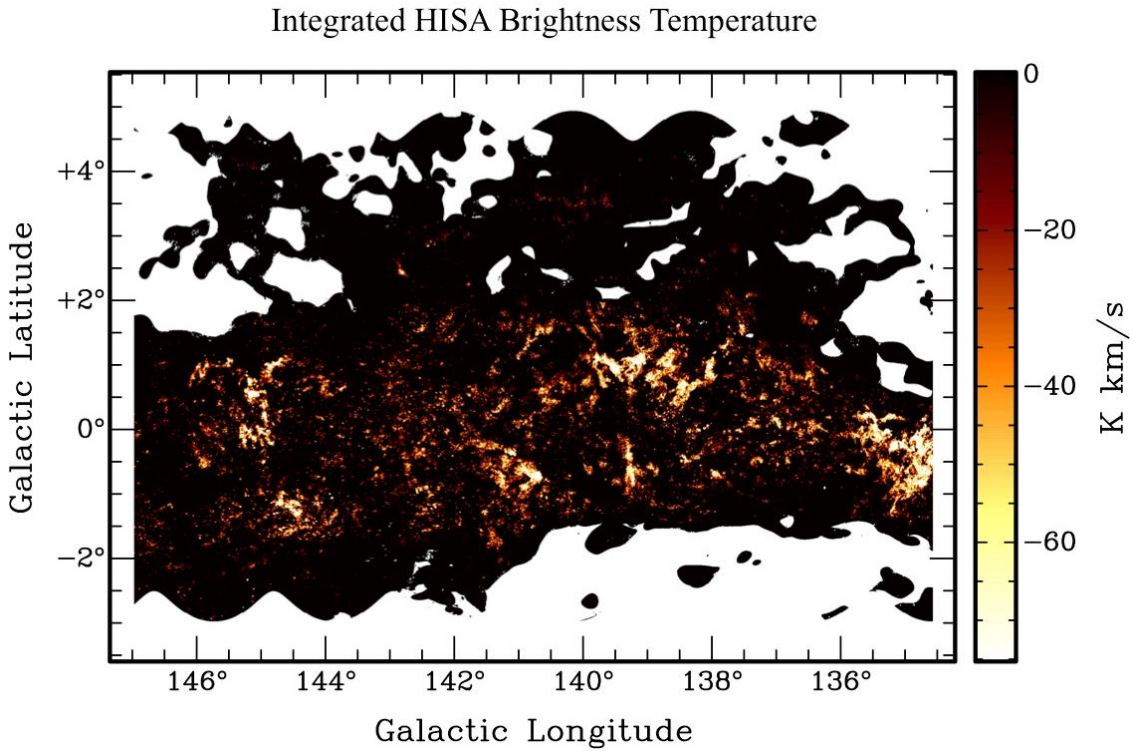

Figure 4. Supermosaic of HISA brightness temperature integrated over velocity. This represents the intensity and location of the HISA features over all of the velocity channels within the CGPS data from which it was extracted using the algorithm of Gibson et al. (2005 a,b). The more negative intensities indicate the presence of more absorption while the blank (white) areas are regions where the algorithm could not determine that HISA was present or not.

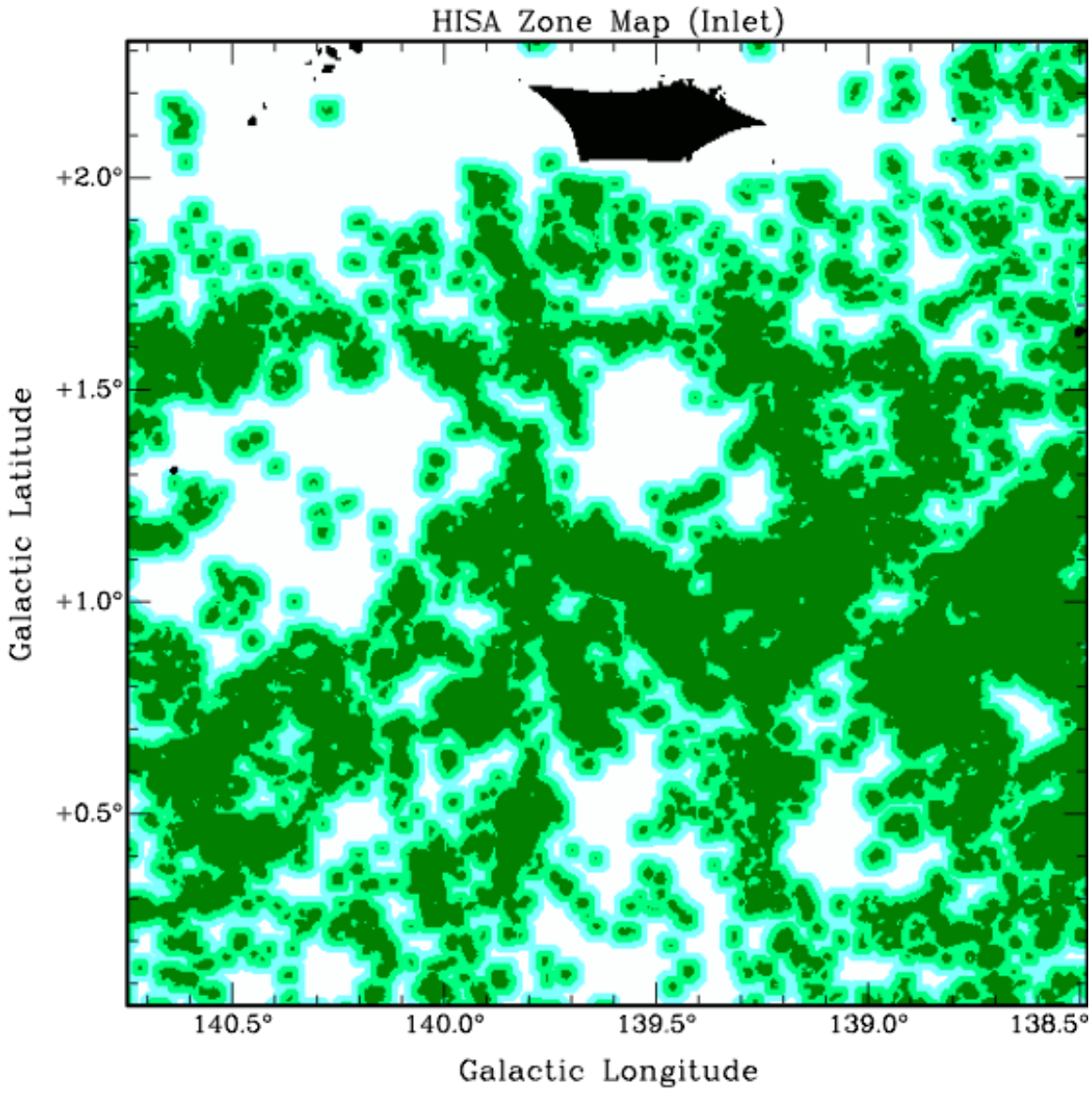

Figure 5. One section of the total supermosaic zone map showing the different regions used in the algorithm. The ON region is dark green and marks where HISA itself is detected and is where all feature measurements are taken. The region immediately contacting the ON region is a buffer zone in which no measurements are taken. This buffer zone is one beam-width wide and compensates for the limitations of the aperture that originally took the CGPS data. The NEAR-OFF region is further out and touches the buffer zone, which should not be HISA but may still contain diffuse H_2. Any other region is OFF and is white in color and represents areas that contain non-blank data that are not contained within any other regions. The black region is a blanked area.

3.3 Interpolation Maps of Observed Gas Tracers

In addition to the surveys providing ON column density values for the HISA clouds, the column densities for the cold, non-HISA gas enveloping the HISA and for the background and adjacent ISM are needed. The material immediately surrounding the HISA should still be very cold and may contain molecules, which is important because it can be used to see what the column density would be if the HISA gas was not present. The NEAR-OFF and OFF regions can be used as references to help determine how much of the total column in the cloud is from visible HI or CO emission, or HISA, or dark H_2.

To do this, interpolation maps must be made for both the dust and CO data, as shown in Figs. 6 and 7 for dust and Figs. 8 and 9 for CO. These interpolation maps are created using the column density maps from Section 2.2 (Figs. 1, 2, and 3) by a computer code separate from the main property algorithm. The interpolation code works by locating pixels associated with HISA regions one at a time and then averaging all OFF pixels within some radius of each ON pixel, weighting this average with a Gaussian function, where *r* is the distance between each OFF pixel and the particular ON pixel. The radius of this circle is dependent on the full-width half-maximum (FWHM), which can be used to derive the (Greek letter sigma) parameter seen in Equation 1. The Gaussian width parameter **σ** can be found from the FWHM with Equation 2.

$$w_i = \exp\left[-\frac{1}{2} \cdot \left(\frac{r_i}{\sigma}\right)^2\right]$$

Equation 1.

$$\sigma = \frac{FWHM}{\sqrt{8 \cdot \ln(2)}}$$

Equation 2.

Since the HISA clouds were originally identified using a spatial filter scale of 20 arc-minutes, this is an obvious first choice for the FWHM of the Gaussian function used in the interpolation. However, trials of the property analysis method have shown that a FWHM of 40 arc-minutes is more reliable since it is a remarkably larger area. A two-fold increase in the interpolation scale guarantees that the more common column densities that are not likely to be associated with erratic, small-scale features and localized behavior will dominate the resulting maps. These artificial features manifest for two reasons: the initial integration of the HISA brightness temperature (Fig. 4) and the introduction of the buffer zones in the zone map (Fig. 5). Both of these factors increase the effective angular size of the HISA features, beyond the original 20 arc-minute resolution is not preserved.

There are other flaws that arise during interpolation as well. Firstly, as is often the case in astronomy, the distances to objects are not precisely known, so we have adopted a single number for the distance in the property code. Second, the *Planck* data used in this study are very likely to be an underestimation of the true total dust column density, and this may be reflected in the interpolation maps. Third, this particular project does not restrict the interpolation to individual HISA clouds and instead uses any region within the area of interpolation, even points in different clouds that may be very different

from one another. Finally, the model used may be oversimplifying cloud structure by assuming that there are no small scale features that are unassociated with the HISA that can cause artificial features to appear in the maps.

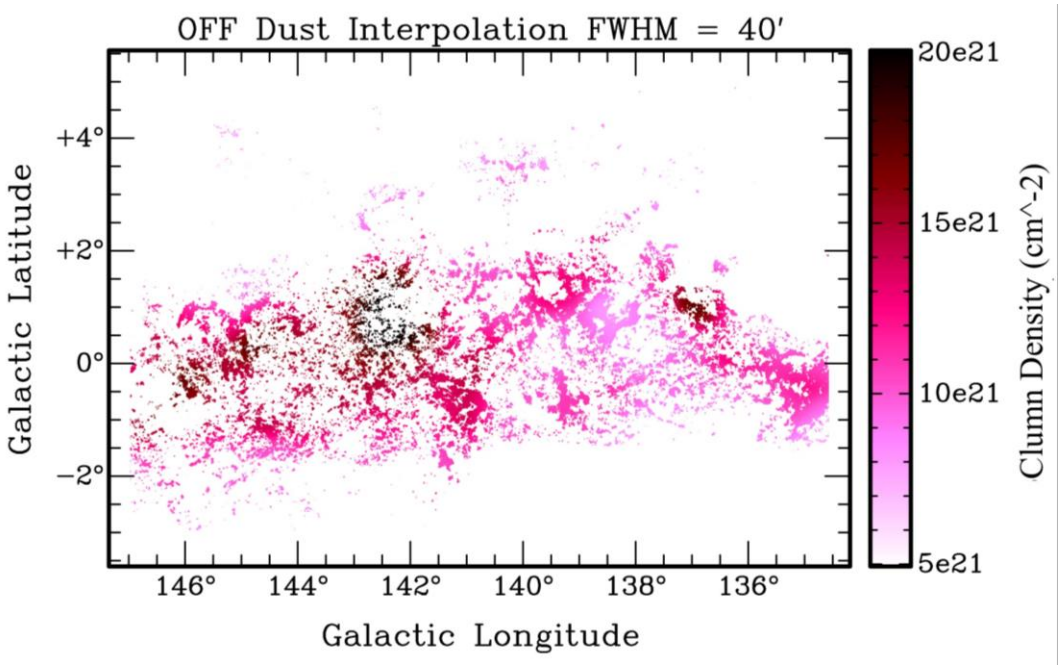

Figure 6. The interpolation map of the OFF dust onto the ON regions. These values are a stand-in for what the dust column density would be if there were no HISA clouds present.

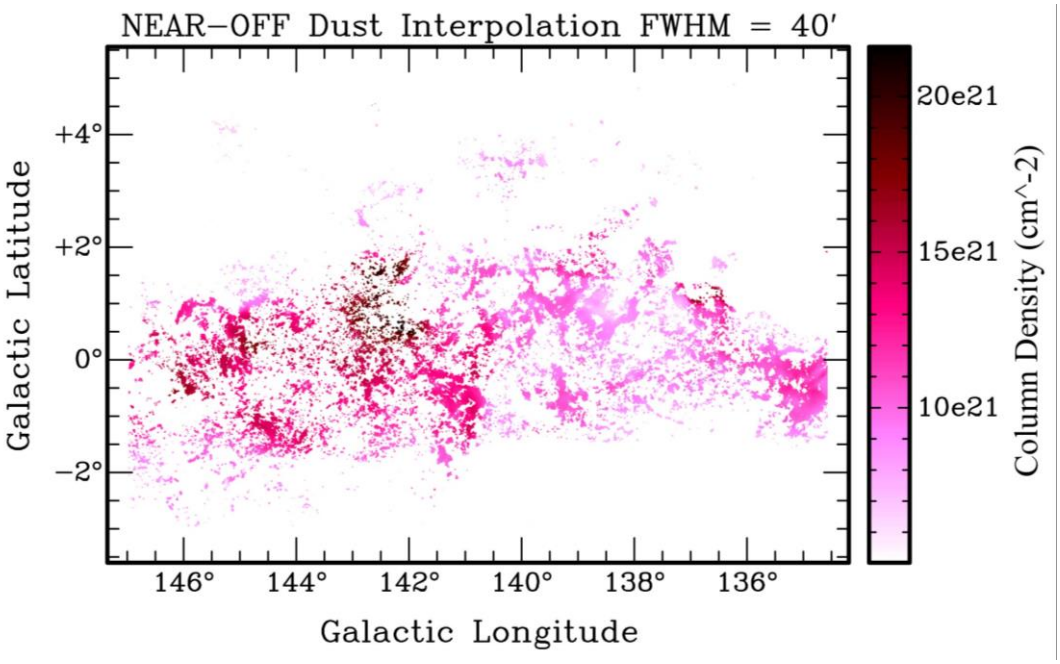

Figure 7. The NEAR-OFF region interpolated onto the ON region. The NEAR-OFF dust column density approximates the column through the cold molecular gas enveloping the HISA, plus background material that is removed later by subtracting the interpolation from the column ON the HISA cloud.

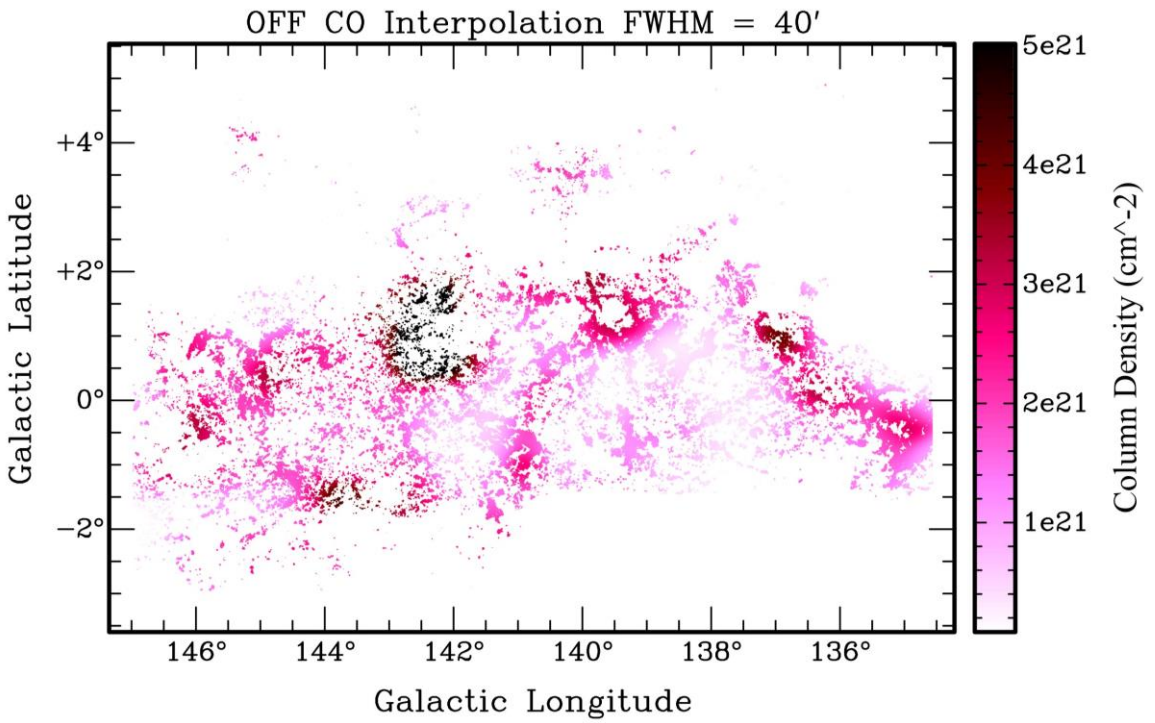

Figure 8. The CO counterpart to Fig. 6 that shows what could have been the background CO column density if the HISA clouds were not present.

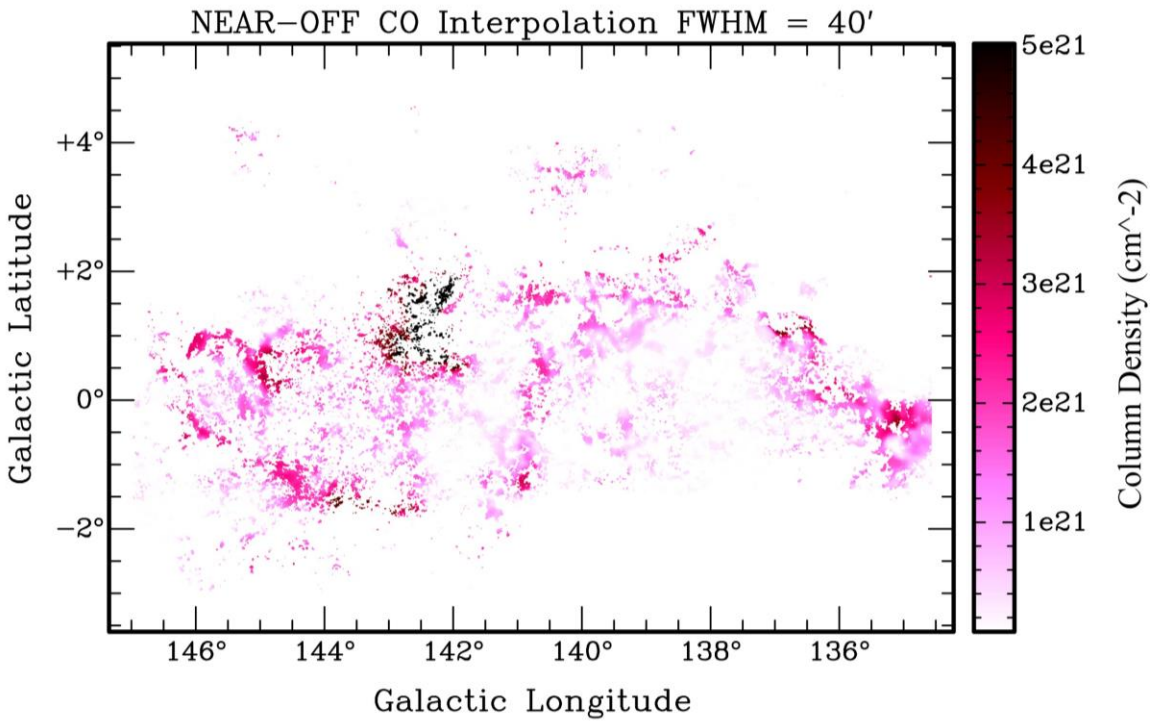

Figure 9. The NEAR-OFF CO column density interpolation map.

3.4 The Property Algorithm

Once the secondary images have been made, the property algorithm itself can be run. The inputs for the algorithm consist of the zone map of the entire region, column density maps, interpolation maps of the the column densities of dust and CO not associated with the HISA cloud and columns associated with the HISA free section of the cold cloud, and file names and locations for the output maps.

When it is run, the algorithm selects HISA features via the zone map and then stores data values from the input images as variables for later use. Applying the rules of radiative transfer and the relationships between the ISM constituents, the algorithm seeks to constrain the upper and lower limits of several physical properties of the HISA clouds. These properties, including temperature, the fractional abundance of atomic to molecular hydrogen, and particle density, can all be determined from a handful of physical assumptions and the column densities of different ISM constituents for the HISA cloud and its associated structures.

The algorithm checks the assumptions of the model: (1) a roughly cylindrical cloud shape, (2) no unrelated dust or CO structures that appear to overlap the HISA cloud but lie elsewhere along the line of sight, and (3) an onion-like structure within the clouds where the inner-most cold center has the highest column density that decreases with distance. While these assumptions are relatively simple, nature can be chaotic and unpredictable, especially the dynamic ISM, so not every HISA cloud may be analyzable with this approach.

After first finding a point associated with a HISA feature, the algorithm will collect the column density values ON the feature and those interpolated from the OFF and NEAR-OFF regions (as mentioned in Sections 3.2 and 3.3) for the three ISM constituents (HI, CO, and dust). There is one caveat with the HI column density maps: it is assumed (Gibson 2005b) that there is no small scale structure in the hydrogen emission, which is reflected in the column density maps because the warmer atomic hydrogen producing most emission is fairly smoothly distributed in space. However, with the CO and dust column density maps, there is no such assumption since molecular clouds tend to be more clumpy. In fact, it is the difference in structure between regions that are and are not associated with the HISA features that make this algorithm possible. Since the CO is a delicate molecule, it will continue to form and persist in regions that are cold and therefore dense, and dust behaves similarly because it traces both HI and H_2. With the essential values (the column densities for the different regions from the data sources) collected by the algorithm, the property calculations can begin.

Many of the preliminary and significant values that are derived are merely the differences of the column densities and serve to isolate certain quantities such as the column density of all neutral hydrogen (atomic and molecular), which is the difference between the dust and CO measurements. By then removing the observable HI column density, that of the untraceable, so called "dark," hydrogen can be found. With this residual column density, a better constraint on the upper and lower limits of the fraction of atomic to molecular hydrogen can be obtained, since the residual value is considered negligible (Gibson 2005b) and not included. The larger the value of f is, the more molecular mate-

rial is present and can be used to account for the hydrogen that has been trapped in a molecular form. The fractional abundance of neutral atomic hydrogen can be found via Equations 3 and 4, which show how the lower and upper limits were derived, respectively:

$$f_L = \frac{N_{DUST} - N_{CO} - N_{DC}}{N_{DUST} - \frac{N_{CO}}{2} - \frac{N_{DC}}{2}}$$

Equation 3

$$f_U = \frac{N_{DUST} - N_{CO} - 0}{N_{DUST} - \frac{N_{CO}}{2} - 0}$$

Equation 4

where N_{DUST} and N_{CO} are the differences between the ON and OFF column densities from the dust or CO data and appropriate interpolation maps. The variable N_{DC} is a stand-in for a similar ON - OFF difference for the total dark hydrogen column, estimated as the difference between the dust and CO column densities. Each f-value limit equation essentially breaks down into the ratio between the HI and the total column density of all neutral H (including the H_2). For the lower limit, the N_{DC} value removes the dust and CO (the tracers for everything but dark H_2), while the dark H_2 is assumed to be zero for the upper limit. These constraints can offer insight into the state of evolution of a particular cloud and whether it is a region where molecules are likely to form.

In addition to the fractional abundance of the hydrogen column densities, the HISA column itself can be found by removing N_{DC} from the difference between the ON

and OFF values of the total dark gas column density in the cloud. Since HISA is cold and not emitting like the warmer background HI, the column density must be found via a method of subtraction. The HISA is the dark HI gas, and this column density can be found by removing the dark molecular material from the total dark hydrogen column, which can easily be obtained by removing the visible HI and CO from the dust column.

This HISA column density can then be used to further limit the spin temperature, which probes the amount by which the cloud is shielded from outside radiation and/or has cooled down, both of which are needed for molecular formation. Equations 5 and 6 show the lower and upper limits of the spin temperature:

$$T_{s,L} = \frac{3000 \cdot f_L \cdot ds_{cm}}{N_{HISA,L}}$$

Equation 5

$$T_{s,U} = \frac{3000 \cdot f_U \cdot ds_{cm}}{N_{HISA,U}}$$

Equation 6

The value 3000 comes from gas thermal pressure divided by the Boltzmann constant and has units of K * cm^{-3}, while ds_{cm} is the estimated distance to the clouds in centimeters (chosen so that the units work out properly).

We can also find the particle density of the HISA from its column density. The particle density differs from the column density in the respect that it is actually a density and has units of cm^{-3} and is needed to understand the rate of molecule formation, since spatially concentrated atoms are more likely to combined together.

The lower and upper limits of the particle density of the HISA can be found with Equations 7 and 8.

$$n_{HISA,L} = \frac{N_{HISA,L}}{ds_{cm}}$$

Equation 7

$$n_{HISA,U} = \frac{N_{HISA,U}}{ds_{cm}}$$

Equation 8

Finally with the particle densities of the HISA, we can find that of all hydrogen with Equations 9 and 10.

$$n_{H,L} = \frac{n_{HISA,L}}{f_L}$$

Equation 9

$$n_{H,U} = \frac{n_{HISA,U}}{f_U}$$

Equation 10

A series of checks were also used within the algorithm to ensure that the input values matched the assumptions in the model. The column densities of the interpolation

maps were compared in a way that the algorithm would proceed only if that of the NEAR-OFF region was larger than the OFF. There was also a control to cancel an individual iteration of the algorithm if some sort of problem in the appropriate column densities (Equations 3 and 4) caused the f-value to be either less than 0 or greater than 1. A comparison between any figure retaining the original HISA cloud outlines (for example, Fig. 9) and the produced property maps shows that this filtered removes many of the HISA clouds where the analysis did not work as intended.

CHAPTER 4

RESULTS

The final products of this process are the collection of property maps. These have the potential to be invaluable tools to be used by astronomers who study the physical properties and state of being of the cold phase of the interstellar medium. Creating these maps to explore how cloud parameters change with location in the Galaxy has always been the goal of this project. This chapter provides some of the output maps whose formulation and generation was described in the section 3.4 along with a summarizing histogram at the end to show which values are most frequent. Some basic observations are made here, while an in-depth discussion will be presented in the Conclusions chapter.

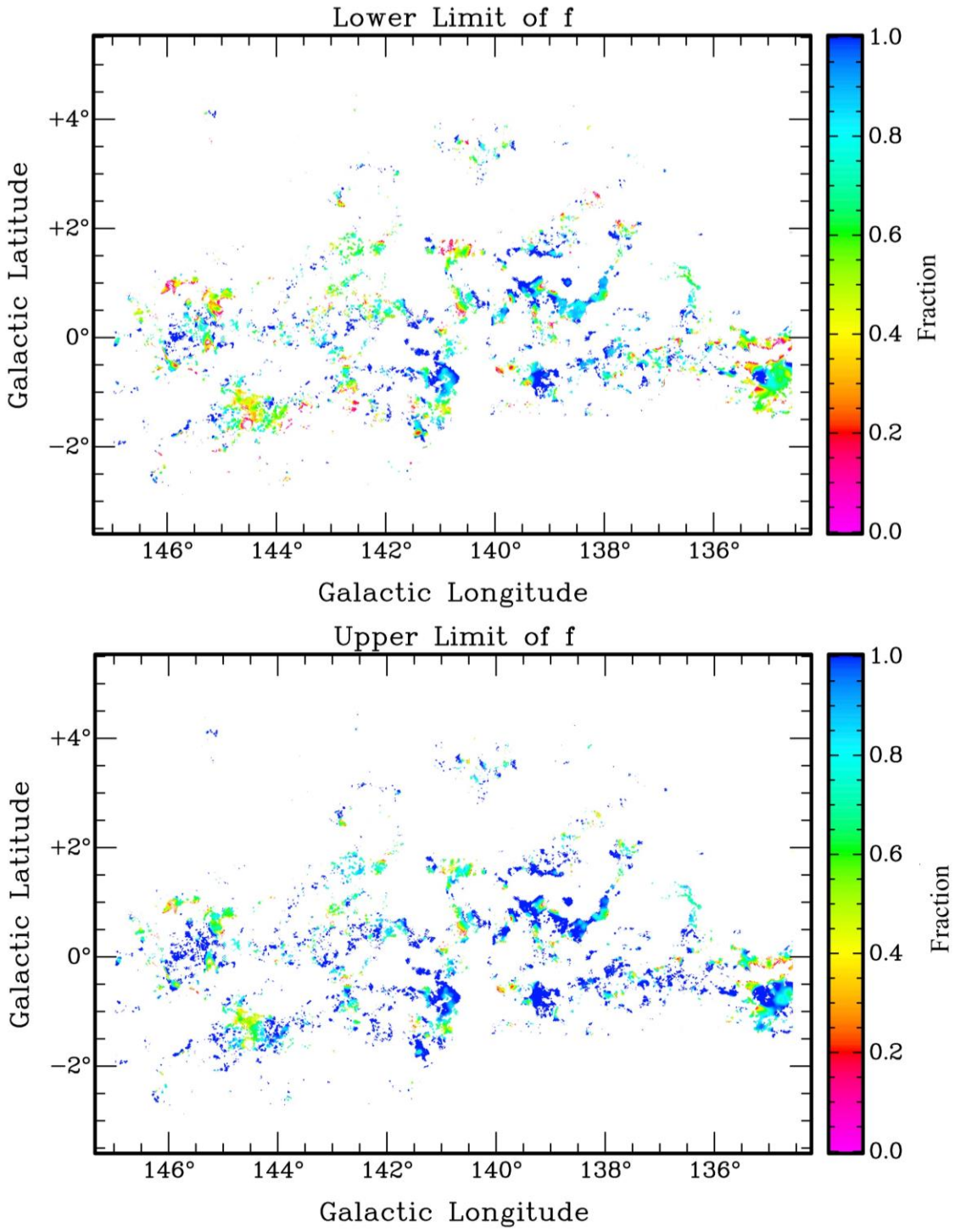

Figure 10. The two maps above show the lower and upper limits for the fraction of atomic hydrogen out of all available hydrogen. For this property, a value closer to 1 indicates mostly atomic hydrogen, while a value close to 0 indicates a cloud that is predominantly molecular in composition.

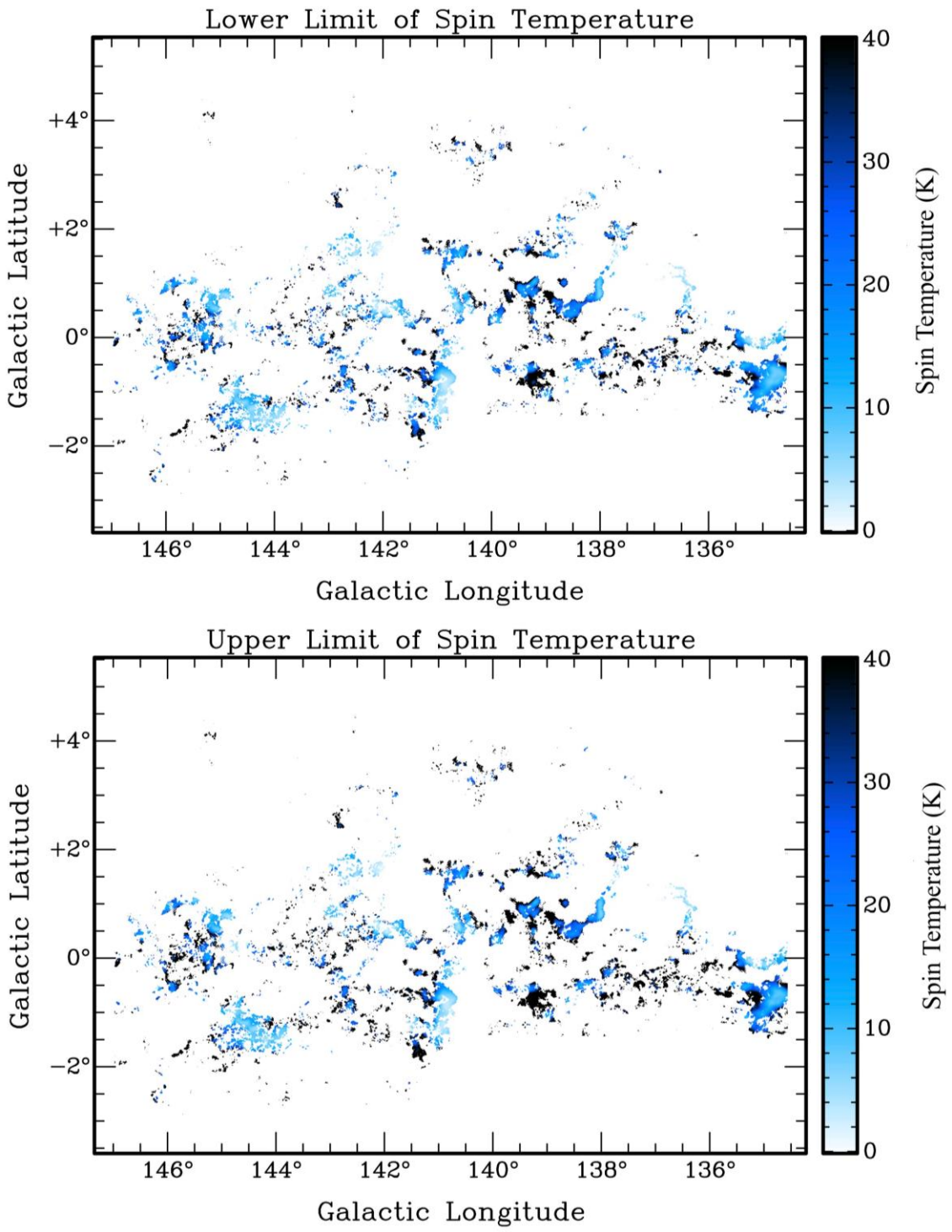

Figure 11. The lower and upper limits for the spin temperature, which is used to gauge how well shielded the cloud is and can offer insight into the molecular content.

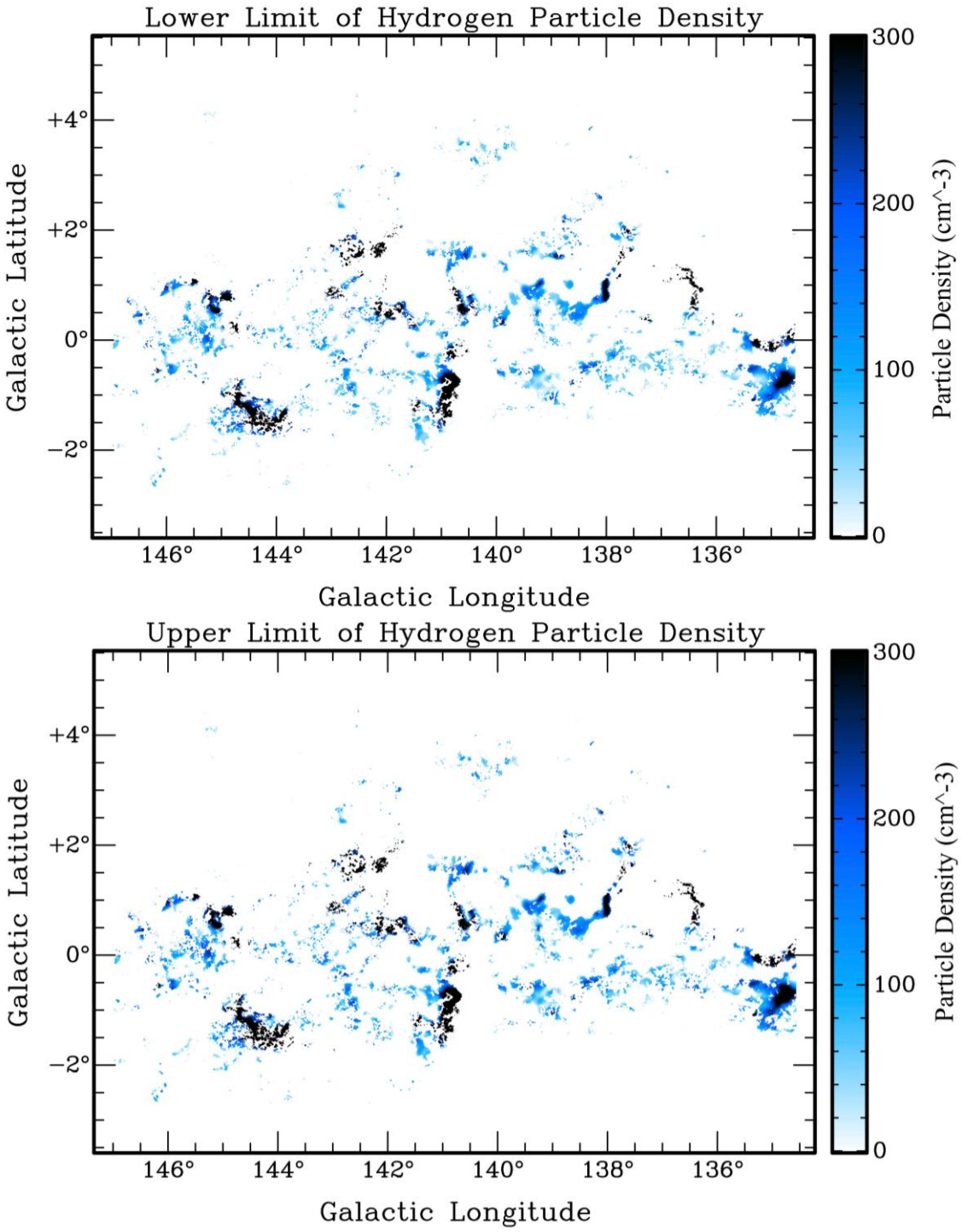

Figure 12. The lower and upper limits on the total hydrogen particle density. This includes both atomic and molecular material that is either observable or dark.

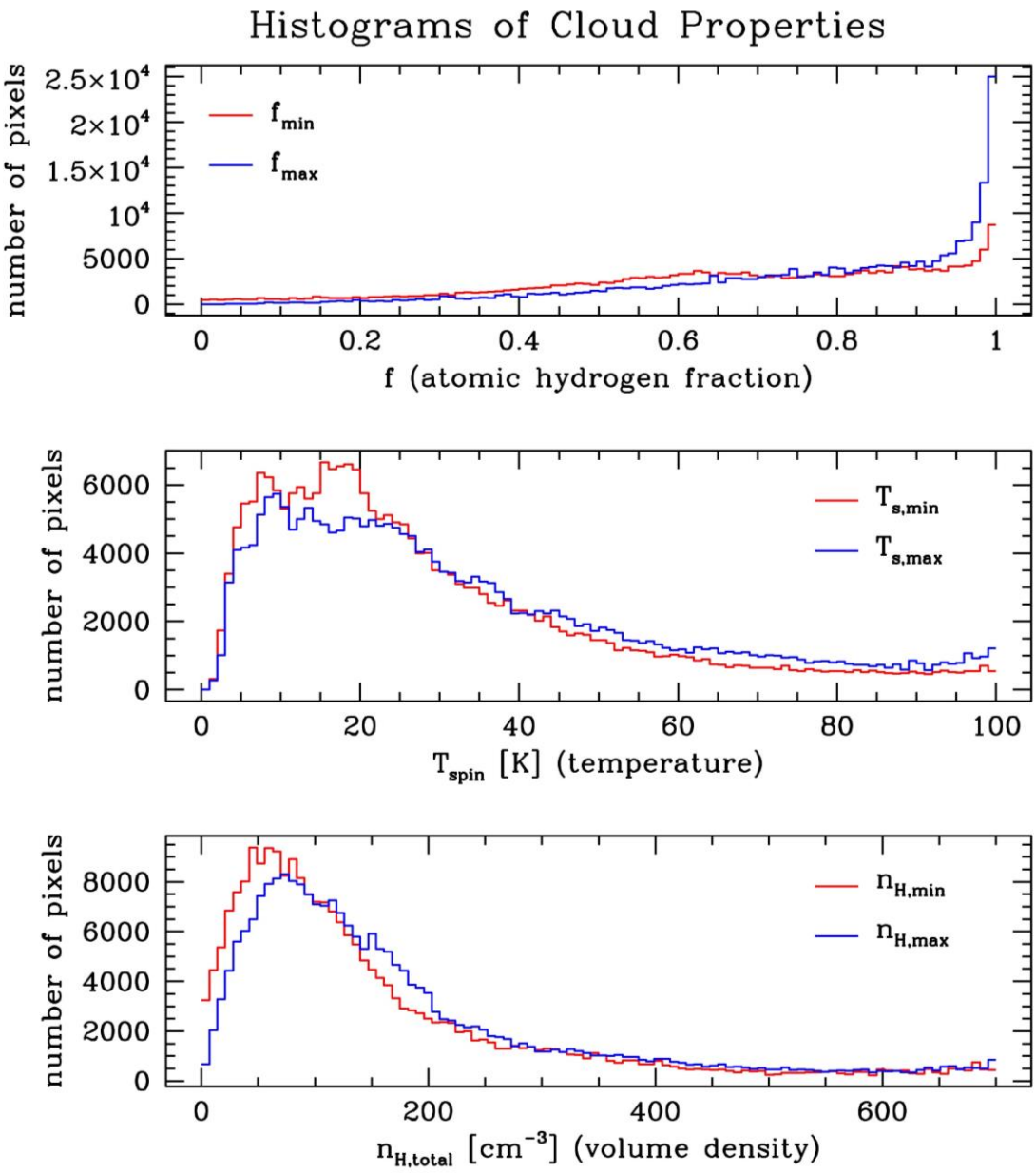

Figure 13. Each of the three histograms above shows the distribution of three properties: the atomic hydrogen fraction, spin temperature, and the total particle density of all hydrogen. The range of each value along the horizontal axis is made up of a total of 100 equally spaced bins.

Fig. 10 is very interesting because both limiting cases have very high f-values, which indicates that most of the gas in the approved target area is atomic rather than molecular. The spin temperature maps in Fig. 11 also show that the gas is very cold, which is unexpected since typical temperatures for the cold neutral phase are ~50 - 100 K (Ferriere 2001). The hydrogen particle densities are around 50 - 75 cm^{-3}, which is consistent with both the cold neutral medium and diffuse H2, as seen in Table 1.

These results are also supported by the histograms in Fig. 13, which show that there is very little variation between the upper and lower limits of the temperature. With the top panel (the histogram for the f-value), there is a large number of pixels in the very highest bins, indicating that these pixels are essentially purely atomic material. This unusual combination of parameters may arise from the clouds transitioning from being atomic to molecular gas.

CHAPTER 5

DISCUSSION

The results presented here provide a thorough test of the analysis method developed for this thesis and are interesting in their own right. The abundance of cold atomic gas suggested by both Figs. 11 and 13 deserves future study; nearby regions in the Galaxy could be given this same treatment to see if similar results are found. These cold temperatures could also be an artifact of the method where troublesomely high or low column densities throw off the f-value, which in turn influences the T_s limits. It is very surprising that the clouds have relatively little spatial structure in their temperature, density, or atomic fraction values: for the most part, the clouds are quite cold and mostly atomic with little variation within. This may mean that the clouds are in a rapid state of evolution, because stable clouds should have the onion-like structure assumed in the model.

This research is very much a work in progress. The testing of new ideas to make the property algorithm more robust has been continuous and shows great promise. As noted in the previous chapter, the analysis sometimes produces bad results, such as atomic gas fractions greater than 1 or negative column densities. These were selectively filtered out to set the corresponding positions blank in the resulting property maps. Additional planned improvements include limiting OFF interpolation pixels to those

whose gas columns are not higher than the group of ON pixels in the cloud in question (Section 3.3), more filtering in the property code itself, ensuring that all images (including the HISA brightness temperature images) have a common resolution of 5 arcminutes, and investigating the use of alternate total column tracers as a check on the *Planck* data with other infrared surveys.

WORKS CITED

Bohlin, R. C., Savage, B. D., & Drake, J. F. 1978, *Astrophysical Journal*, 224, 132

Carroll, B. W., & Ostlie, D. A. 2007, *An Introduction to Modern Astrophysics* (Pearson Addison-Wesley)

Dame, T. M., Hartmann, D., & Thaddeus, P. 2001, *Astrophysical Journal*, 547, 792

Dickey, J. M., & Lockman, F. J. 1990, *Annual Reviews of Astronomy & Astrophysics*, 28, 215

Douglas, K. A., & Taylor, A. R. 2007, *Astrophysical Journal*, 659, 426

Draine, B. T. 2011, *Physics of the Interstellar and Intergalactic Medium* (Princeton: Princeton University Press)

Feldt, C. 1993, *Astronomy & Astrophysics*, 276, 531

Ferriere, K. M. *Review of Modern Physics*, 73, 1031

Gibson, S. J., Taylor, A. R., Dewdney, P. E., & Higgs, L. A. 2000, *Astrophysical Journal*, 540, 851

Gibson, S. J., Taylor, A. R., Higgs, L. A., Dewdney, P. E., & Brunt, C. M. 2005a, *Astrophysical Journal*, 626, 214

Gibson, S. J., Taylor, A. R., Higgs, L. A., Dewdney, P. E., & Brunt, C. M. 2005b, *Astrophysical Journal*, 626, 195

Gibson, S. J. 2010, *Astronomical Society of the Pacific Conference Series*, 438, eds. R. Kothes, T. L. Landecker, & A. G. Willis (San Francisco: ASP), 111

Grenier, I. A., Casandjian, J.-M., & Terrier, R. 2005, *Science*, 307, 1292

Heyer, M. H., Brunt, C., Snell, R. L., Howe, J. E., Schloerb, F. P., & Carpenter, J. M. 1998, *Astrophysical Journal Supplement*, 115, 241

Kavars, D. W., Dickey, J. M., McClure-Griffiths, N. M., Gaensler, B. M., & Green, A. J. 2003, Astrophysical Journal, 598, 1048

Planck Collaboration (corresponding author: J. A. Tauber) 2014, Astronomy & Astrophysics, 571, 1

Taylor, A. R., Gibson, S. J., Peracaula, M., & et al. 2003, Astronomical Journal, 125, 3145